Mem. S.A.It. Vol. 74, 635

Memorie della

Spatially resolved signatures of chromospheric evaporation during a small two-ribbon flare

L. Teriaca[1] ⋆, A. Falchi[1], G. Cauzzi[1], R. Falciani[2], L.A. Smaldone[3] and V. Andretta[4]

[1] INAF-Osservatorio Astrofisico di Arcetri, 50125 Firenze, Italy
e-mail: lte@arcetri.astro.it
[2] Dipartimento di Astronomia e Scienza dello Spazio, Università di Firenze, 50125 Firenze, Italy
[3] Dipartimento di Scienze Fisiche, Università di Napoli "Federico II", 80126 Napoli, Italy
[4] Osservatorio Astronomico di Capodimonte, 80131 Napoli, Italy

Abstract. Ground based spectroheliograms of a solar active region were acquired in four chromospheric lines simultaneously with rasters in transition region (TR) and coronal lines obtained with the Coronal Diagnostic Spectrograph (CDS) aboard SOHO. Such a complete dataset allows us to study the development of intensity and velocity fields during a small two-ribbon flare in the whole atmosphere. In particular, we obtain for the first time quasi-simultaneous and spatially resolved observations of velocity fields during the impulsive phase of a flare, both in chromosphere and upper atmosphere. In this phase, strong downflows (up to 40 km s^{-1}) following the shape of the developing ribbons are measured at chromospheric levels, while strong upward motions are measured in TR (up to -100 km s^{-1}) and coronal lines (-160 km s^{-1}). The spatial pattern of these velocities have a common area about 10 arcsec wide. This is the first time that opposite directed flows at different atmospheric levels are observed in the same spatial location during a flare. These signatures are highly suggestive of the chromospheric evaporation scenario predicted in theoretical models of flares.

Key words. Solar activity – Flares – Atmospheric motions

1. Introduction

Blue-shifted emission in coronal lines (e. g. Antonucci et al. 1982) and red-shifted emission in chromospheric lines (e. g. Ichimoto & Kurokawa 1984) has been observed during the impulsive phase of flares. These shifts have been interpreted respectively as coronal up-flows up to 400 km

Send offprint requests to: L. Teriaca
⋆ now at Max Planck Institut für Aeronomie, D-37191 Katlenburg-Lindau, Germany
Correspondence to: Osservatorio Astrofisico di Arcetri, Largo Enrico Fermi 5, 50125 Firenze, Italy

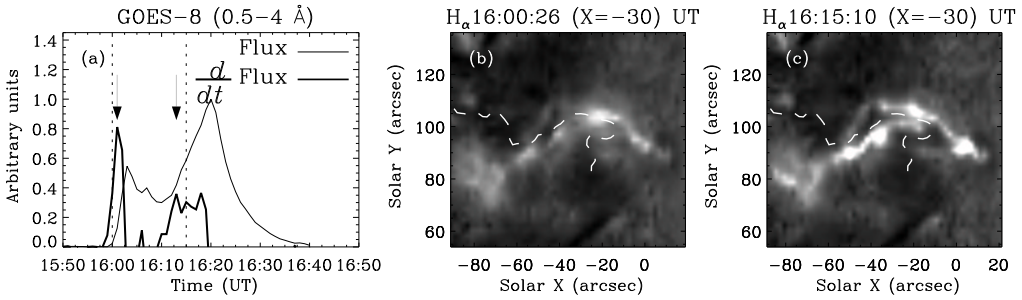

Fig. 1. *a*: Soft X-ray full disk flux at 1 AU in the 0.5−4 Å band (solid thin line) around the time of the flare. The time derivative (solid thick line) represents a proxy for the hard X-ray curve. Main local maxima in the derivative ($\sim$ 16 : 01 and $\sim$ 16 : 13 UT) are marked by arrows. Dotted vertical lines marks the times at which the Hα images on panels *b* and *c* were obtained. The white dashed lines on *b* and *c* (and in Fig. 2) mark the magnetic neutral line obtained from a MDI magnetogram acquired at 16:00 UT.

s^{-1}, and chromospheric down-flows up to 100 km s^{-1}, and can be explained through hydrodynamic simulations of the so-called "explosive chromospheric evaporation", a sudden increase of the chromospheric temperature to coronal values, occurring when the chromospheric plasma is heated beyond its ability to radiate (Nagai & Emslie 1984; Fisher 1986; Gan et al. 1991). In these models the overpressure of the chromospheric evaporated plasma is responsible for the dynamics of the flare. Thus, the momentum of downward moving plasma (e.g. observed in Hα) should be equal to the momentum of the upflowing coronal plasma. Moreover, upward and downward motions should be observed at the same location. Although the equality of the two momenta during the impulsive phase has been proved within a factor of 2-6 for a few events (see e. g. Canfield et al. 1990), it must be noted that in these cases the coronal observations were spatially unresolved. Up to now, only indirect observational proofs on the spatial coincidence of coronal upflows and chromospheric downflows have been provided (Wülser et al. 1994).

Here we present coordinated observations of a small two-ribbon flare, developing in region NOAA 9468 on 2001 May 26 around 16 UT (cosθ=0.99). These observations, combining spatially resolved spectral observations with quasi-simultaneously measurements in the chromosphere and the upper atmospheric layers, seems particularly suitable to shed some light on the problem.

2. Observations

CDS Data: Raster scans in He I 584 (log T=4.3), He II 304 (log T=4.8), O V 630 (log T=5.4), Fe XVI 360 (log T=6.3), and Fe XIX 592 Å (log T=6.9) were obtained with the CDS-Normal Incidence Spectrometer on a final useful field of view (FOV) of 148″ × 138″, with a spatial resolution of 6″×3.4″/pixel. Temporal cadence was $\sim$ 14 s/slit position, and a full raster scan took about 5.5 min.

DST Data: Several chromospheric lines were monitored with the Horizontal Spectrograph at the Dunn Solar Telescope (DST): Ca II-K, Hα, He I 5876 Å (D3) and He I 10830 Å. The final FOV was of 160″ × 140″, with a spatial resolution of 2″ × 2″. Spectra at each slit position were recorded in 3.5 s, and a full raster scan of the AR took about 5 m.

3. Flare development

Although very small (C1.1 class) this flare displays all the characteristics of an eruptive flare. Its evolution is summarized by Fig. 1. Panel *a* shows the soft X-ray (SXR) flux in the 0.5 - 4 Å range provided by the GOES-8 satellite. Since no hard X-ray (HXR) measurement was available for this flare, we used the time-derivative of the SXR flux as a proxy for the HXR emission, as discussed by Dennis & Zarro (1993). Two rapidly developing flare ribbons appear on either side of the magnetic neutral line at the time of the first HXR peak (Fig. 1*b*). At this time, the ribbons are still very close to the magnetic neutral line. A second major episode of energy release occurred around 16:13 UT. At both chromospheric and TR level, this phase is characterized by the brightening of different kernels in the flaring ribbons. The ribbons are expanding farther away from the magnetic neutral line and appear now clearly separated (Fig. 1*c*).

As typical of eruptive flares, the decay phase extended for a fairly long period (more than 40 minutes from the second soft X-ray peak, see Fig. 1*a*), with successive episodes of energy release that affected portions of the ribbons farther away from the neutral line.

4. Velocity patterns at flare peak

During the flare initial phase, strong downflows (30-40 km s^{-1}) following the shape of the developing ribbons are measured in He I 10830 in the raster acquired around 16:05 UT. They are shown as black solid contours in Fig. 2, overlaid on the relative Hα spectroheliogram. Strong upward motions are instead measured in O V around 16:02:30 UT, with values reaching 100 km s^{-1}. As one can see from Fig. 2, the TR upflows and chromospheric downflows are spatially coincident over the area of the maximum O V velocity. This is the same area, $\approx 10''$ wide, where upflows of about -160 km s^{-1} are measured at the same time in the Fe XIX 592 coronal line.

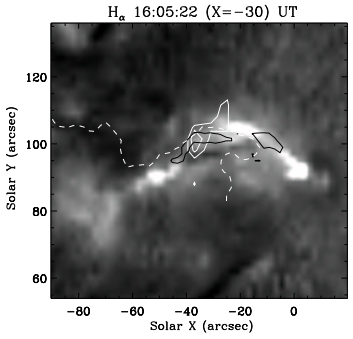

Fig. 2. Velocity contours of He I 10830 downflows measured around 16:05:14 UT (+25 km s^{-1}, black solid lines), overlaid on the simultaneous image in Hα. Isocontours of the velocities measured around 16:02 UT by CDS in the O V 630 (-80, -60 km s^{-1} – white solid lines) are also shown.

Fig. 3*a* shows the He I 10830 profile averaged on the active region before the start of the flare (thin line) and in the flaring point where maximum upward velocities are measured in O V (thick line). The flare profile, although still in absorption, is much stronger than the quiet case, and clearly shows a red-shifted component. In Fig. 3*b* we show the O V profile from which maximum upward velocity (~ -100 km s^{-1}) is measured at 16:02:30 UT (thick solid line) around X= $-37''$, Y= $101''$, together with the profile obtained averaging the entire scan preceding the flare onset (thin solid line). Fe XIX profiles significantly diverging from the reference profile are visible only at 16:02 UT around the location of maximum O V blue-shifts. The line profiles obtained averaging over the same CDS points at the four successive scans (from 16:08:14 to 16:25:21 UT) are instead identical in width and position and their average was used as a reference profile (thin dashed line in Fig. 3*c*). A multi component fitting was hence applied to the 16:02 UT profile, constraining the rest component by imposing width and position of the reference pro-

file, while the background (thin dot-dashed line in Fig. 3*c*) was constrained through the average non-flare spectrum. A blue-shifted component (thin dotted line in Fig. 3*c*) is now evident, yielding an upward directed velocity of -160 ± 70 km s^{-1}.

This is the first time that quasi-simultaneous and opposite directed motions in different atmospheric layers are observed in the same spatial location during a flare. Given the temporal delay between the CDS and DST measurements with respect to the typical duration of impulsive motions at both coronal and chromospheric levels (30-90 s, Antonucci 1989; Ichimoto & Kurokawa 1984), we are most probably not observing the same flaring episode. However, it is well known that during the development of two-ribbon flares magnetic reconnection and its associated effects, such as impulsive flows, occur repeatedly in very close spatial positions (Forbes & Acton 1996; Falchi et al. 1997; Czaykowska et al. 1999), so it seems plausible that we are witnessing distinct events within the same area. These signatures are highly suggestive of the chromospheric evaporation scenario predicted in theoretical models of flares.

Acknowledgements. The work of L.T. has been supported by ASI and MIUR. We thank the NSO/SP and CDS teams.

References

Antonucci, E. et al. 1982, Sol. Phys. 78, 107
Antonucci, E. 1989, Sol. Phys. 121, 31
Canfield, R.C. et al. 1990, ApJ 348, 333
Czaykowska, A. et al. 1999, ApJ 521, L75
Dennis, B.R. & Zarro, D.M. 1993, Sol. Phys. 146, 177
Falchi, A. et al. 1997, A&A 328, 371
Fisher, G.H. 1986, Lecture Notes in Phys. 255, 53
Forbes, T.G. & Acton, L.W. 1996, ApJ 459, 330
Gan, W.Q. et al. 1991, A&A 241, 618
Ichimoto, K. & Kurokawa, K. 1984, Sol. Phys. 93, 105
Nagai, F. & Emslie, A.G. 1984, ApJ 279, 896

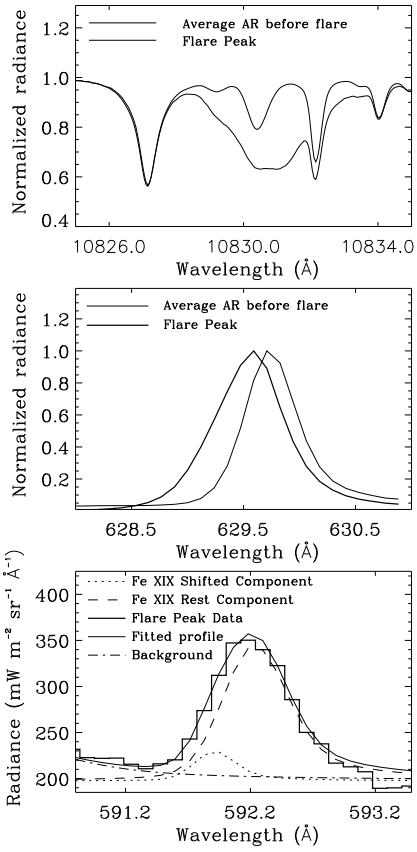

Fig. 3. He I 10830, O V 630 and Fe XIX 592 Å line profiles observed at flare peak (thick solid lines) in the location of maximum O V blueshift. *(a)* Average He I 10830 active region line profile before flare (thin solid line) together with the flare peak profile. *(b)* Normalized O V flare line profile together with the average line profile obtained before the flare (thin solid line). *(c)* Fe XIX flare profile (thick solid histogram) together with the fitted profile (thin solid line). Thin dashed line represents the rest component, while the thin dotted line shows the blueshifted component. Thin dot-dashed line marks the fitted background.

Wülser, J.P., et al. 1994, ApJ 424, 459